... were described by Aristotle as early as the fourth century B.C. In their Communication on page 8124 ff., I. V. Yampolsky, J. I. Gitelson, and co-workers unveil the structure of fungal luciferin, a compound that is responsible for fungal biolumescence.

Cancer Diagnostics

A hypoxia-sensitive sensor for tracking cancer metastasis is reported by X. Q. Jiang et al. on page 8094 ff. After systemic administration of the sensor, cancer cells metastasizing to the lungs or to the lymph nodes are detected by whole-body optical imaging.

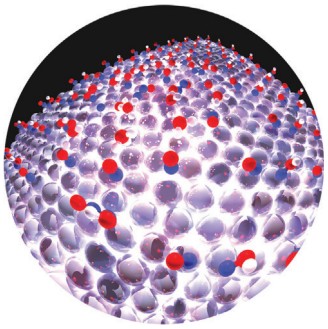

NO Electroreduction

The crucial role of water in determining the mechanism of NO electroreduction to ammonia on Pt(111) surfaces is investigated by J. Greeley et al. in their Communication on page 8255 ff. Water facilitates proton transfer to adsorbed surface intermediates with very low kinetic barriers.

Porphyrinoids

M. Bröring et al. present the first free-base corrole radical in their Communication on page 8213 ff. Loss of an inner hydrogen atom from the air-stable, easy-to-handle porphyrinoid gives a planar molecule that can, for example, bind Zn^{2+}.

How to contact us:

Editorial Office:
E-mail: angewandte@wiley-vch.de
Fax: (+49) 62 01–606-331
Telephone: (+49) 62 01–606-315

Reprints, E-Prints, Posters, Calendars:
Carmen Leitner
E-mail: chem-reprints@wiley-vch.de
Fax: (+49) 62 01–606-331
Telephone: (+49) 62 01–606-327

Copyright Permission:
Bettina Loycke
E-mail: rights-and-licences@wiley-vch.de
Fax: (+49) 62 01–606-332
Telephone: (+49) 62 01–606-280

Online Open:
Margitta Schmitt, Carmen Leitner
E-mail: angewandte@wiley-vch.de
Fax: (+49) 62 01–606-331
Telephone: (+49) 62 01–606-315

Subscriptions:
www.wileycustomerhelp.com
Fax: (+49) 62 01–606-184
Telephone: 0800 1800536 (Germany only)
+44(0) 1865476721 (all other countries)

Advertising:
Marion Schulz
E-mail: mschulz@wiley-vch.de
jspiess@wiley-vch.de
Fax: (+49) 62 01–606-550
Telephone: (+49) 62 01–606-565

Courier Services:
Boschstrasse 12, 69469 Weinheim

Regular Mail:
Postfach 101161, 69451 Weinheim

Angewandte Chemie International Edition is a journal of the Gesellschaft Deutscher Chemiker (GDCh), the largest chemistry-related scientific society in continental Europe. Information on the various activities and services of the GDCh, for example, cheaper subscription to *Angewandte Chemie International Edition*, as well as applications for membership can be found at **www.gdch.de** or can be requested from GDCh, Postfach 900440, D-60444 Frankfurt am Main, Germany.

GDCh
Gesellschaft Deutscher Chemiker

Editorial

"... There is more than what meets the eye. After 25 years of optical experiments on single molecules, it is time to reflect on the insights and the present or potential applications that single-molecule optics, and more generally single-molecule chemistry, have brought to us. Subtle and detailed information can be gleaned from the wealth of signals single molecules relay to us from their nanometer-scale environment ..."
Read more in the Editorial by Michel Orrit.

Service

Author Profile

"I admire dedication and true achievement—in all areas of life.
My favorite way to spend a holiday is motorcycling (or skiing, depending on the season) in the Alps ..."
This and more about Albrecht Berkessel can be found on page 8028.

News


K. Matyjaszewski


E. P. Balskus


W. Min


D. A. Nicewicz


J. A. Prescher

Books

Nobel Lectures

Super-Resolution Microscopy

The resolution of a microscope is determined by the diffraction limit in classical microscopy, whereby objects that are separated by half a wavelength can no longer be visually separated. To go below the diffraction limit required several tricks and discoveries. In his Nobel Lecture, E. Betzig describes the developments that have led to modern super high-resolution microscopy.

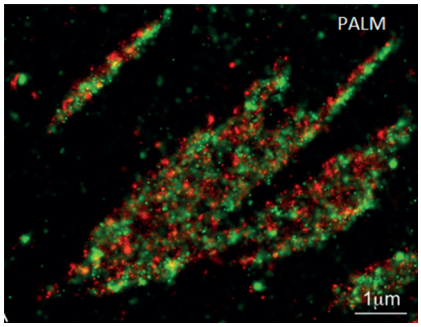

Super-Resolution Microscopy

A picture is worth a thousand words—This doesn't only apply to everyday life but also to the natural sciences. It is, therefore, probably not by chance that the historical beginning of modern natural sciences very much coincides with the invention of light microscopy. S. W. Hell shows in his Nobel Lecture that the diffraction resolution barrier has been overcome by using molecular state transitions (e.g. on/off) to make nearby molecules transiently discernible.

Super-Resolution Microscopy

In the early 90s, many fascinating physical effects were observed when ensemble averaging was removed to allow study of individual molecules. The imaging of single molecules as well as observations of spectral diffusion, optical switching, and the ability to select different single molecules in the same focal volume by tuning the pumping laser frequency provided important forerunners of the later super-resolution microscopy with single molecules.

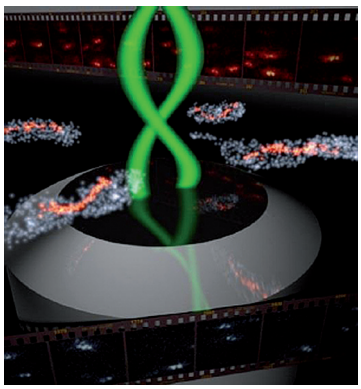

For the USA and Canada:
ANGEWANDTE CHEMIE International Edition (ISSN 1433-7851) is published weekly by Wiley-VCH, PO Box 191161, 69451 Weinheim, Germany. US mailing agent: SPP, PO Box 437, Emigsville, PA 17318. Periodicals postage paid at Emigsville, PA. US POSTMASTER: send address changes to *Angewandte Chemie*, John Wiley & Sons Inc., C/O The Sheridan Press, PO Box 465, Hanover, PA 17331. Annual subscription price for institutions: US$ 11.738/10.206 (valid for print and electronic / print or electronic delivery); for individuals who are personal members of a national chemical society prices are available on request. Postage and handling charges included. All prices are subject to local VAT/sales tax.

Communications

Tracking down cancer: A hypoxia-sensitive optical oxygen nanosensor is reported for tracking cancer metastasis in vivo. After systemic administration of the nanosensor, cancer cells metastasizing to the lungs through the blood stream or to the lymph node through lymphatics can be effectively detected by whole-body optical imaging.

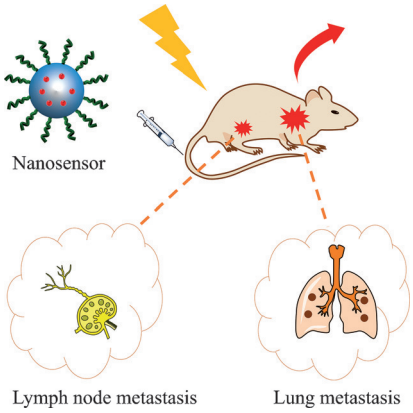

Cancer Diagnostics

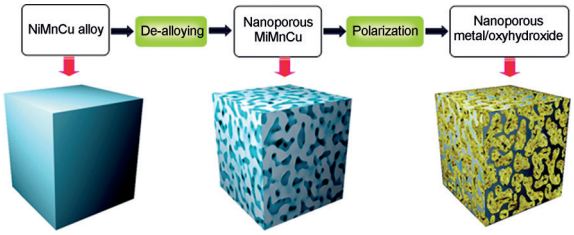

Electrochemical polarization of a de-alloyed nanoporous NiCuMn alloy was employed to synthesize a novel multi-component mixed-valence oxyhydroxide based electrode. The oxyhydroxide/metal electrode possesses both high specific capacitance (627 $F\,cm^{-3}$) at a current density of 0.25 $A\,cm^{-3}$ and a wide working-potential window (1.8 V) in aqueous electrolyte, thereby resulting in a high energy and power densities with excellent cyclic stability.

Electrochemistry

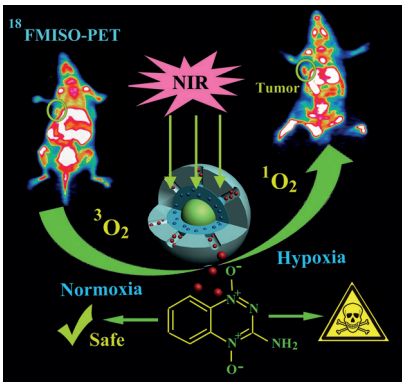

Synergetic therapy: Strong hypoxia created by upconversion photodynamic therapy (UC-PDT) activates bioreductive pro-drugs co-delivered to form cytotoxic species, thereby potentiating the synergetic anticancer efficacy of UC-PDT. This process was accomplished by using upconversion-based nanoparticles designed to simultaneously deliver photosensitizer molecules and bioreductive pro-drugs in silica layers.

Nanotechnology

Electrochemistry

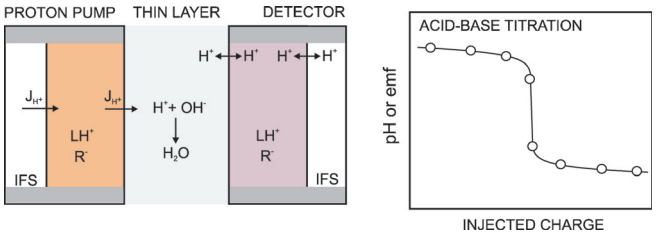

A chemically selective electrochemical proton pump creates a concentration perturbation in a thin-layer sample that is detected by a pH probe placed opposite. The proposed methodology is applicable for a range of ions and is demonstrated here for direct alkalinity measurements. L = ionophore; R^- = cation exchanger; J_{H+} = proton flux; IFS = inner filling solution.

Gold Nanoparticles

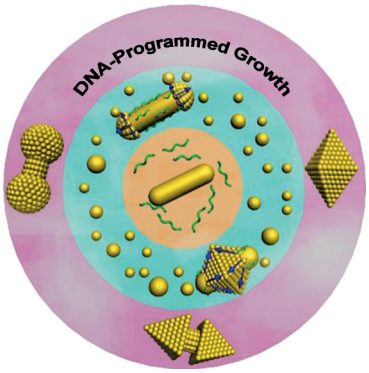

Controlling nanoparticle morphology was achieved by tuning the overgrowth of gold nanorods using DNA as a capping ligand. Kinetic studies show two representative pathways for the shape control. Furthermore, the geometric and plasmonic properties of the gold nanoparticles could be precisely controlled by adjusting the base composition of the DNA sequences or by introducing phosphorothioate modifications in the DNA.

Biocatalytic Self-Assembly

Off the beaten track: Sequence-dependent kinetic pathway selection in chemically fueled catalytic self-assembly of tripeptides is demonstrated, in which the control of the lifetime of the nanostructures is dictated by chemical design. Mimicking the unique features of these systems may open up opportunities to create supramolecular systems for non-equilibrium motility and shape control.

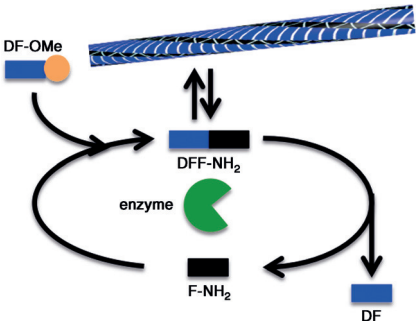

Bioluminescence

Front Cover

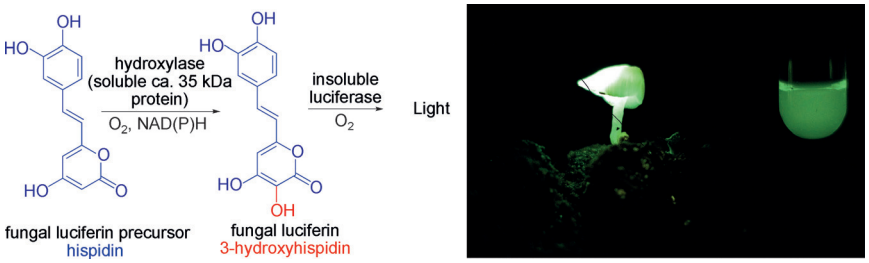

Getting the green light: Hispidin is shown to be a luciferin precursor in at least four evolutionary distant genera of luminous fungi. However, its biosynthesis alone does not result in fungal bioluminescence. Two enzymes are required: first a hydroxylase converts the hispidin into 3-hydroxyhispidin, which acts as the luciferin, which undergoes a subsequent oxidation in the presence of a luciferase.

Protein Dynamics

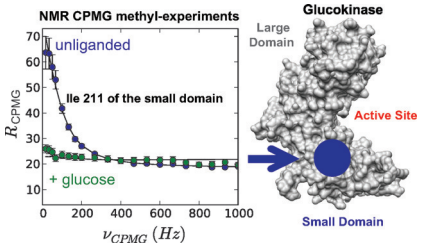

Distant but decisive: Kinetic cooperativity is an intrinsic property of glucokinase that enables it to maintain whole-body glucose homeostasis. The small-domain dynamics of glucokinase on the millisecond timescale have now been quantified by NMR spectroscopic experiments and found to be responsible for this effect by interfering with the turnover rate constant and generating non-Michaelis–Menten kinetics (see picture).

Semiconducting Nanostructures

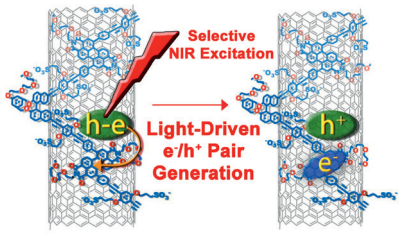

Nanohybrid compositions based on (6,5) chirality-enriched SWNTs and a chiral n-type polymer (*S*-PBN(b)-Ph_4PDI) that exploits a perylenediimide-containing repeat unit undergo light-driven electron–hole pair generation. Rigorously controlled SWNT:electron acceptor stoichiometry and organization enable spectroscopic characterization of the photoinduced charge carrier signatures and evaluation of the associated charge separation and charge migration dynamics by pump-probe transient absorption spectroscopy.

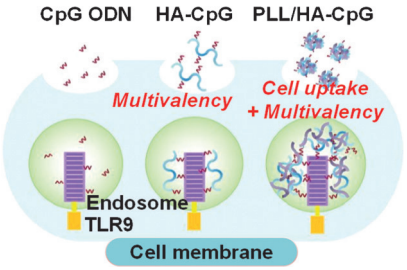

Enhanced immunostimulation: A multivalent polymer nanocomplex for the effective intracellular delivery and subsequent multivalent display of immunostimulatory cytosine-phosphate-guanine oligodeoxynucleotides (CpG ODNs) in antigen-presenting cells is described. Mice vaccinated with dendritic cells treated with the nanocomplex exhibited tumor growth inhibition as well as a strong antitumor memory response. HA = hyaluronic acid, PLL = poly-(L-lysine).

Multivalent Polymer Nanocomplex

DNA branches out: A hyperbranched hybridization chain reaction is reported for the self-assembly of dendritic DNA structures triggered by an initiator DNA strand. By using this method, ultrasensitive detection of target DNA was achieved and three-input concatenated logic circuits have been constructed which can operate as keypad locks for biocomputing security systems at the molecular level.

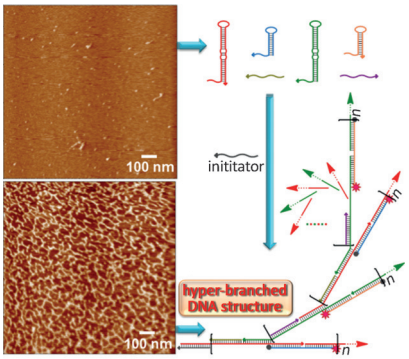

DNA Self-Assembly

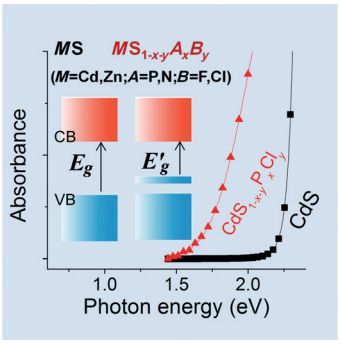

Anionic doping: Cosubstitution of CdS and ZnS by P, Cl and N, F brings about remarkable changes in the electronic structure of these materials as the electronic band gaps are significantly decreased (E_g = band-gap energy). The effect of both P, Cl and N, F in CdS and ZnS were studied by DFT calculations, and the changes were measured by high-resolution X-ray photoelectron spectroscopy.

Photocatalysis

Unbiased selection: A kinase inhibitor screening approach was developed that uses a radically different basis of detection than existing methods. Engineered protein nanopores allow the label-free determination of inhibition constants, are scalable to high-throughput, and circumvent biases inherent in prevailing technologies.

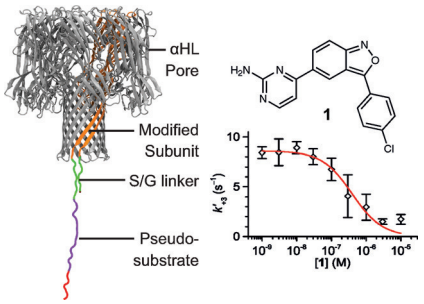

Drug Screening

Chiral Borospherenes

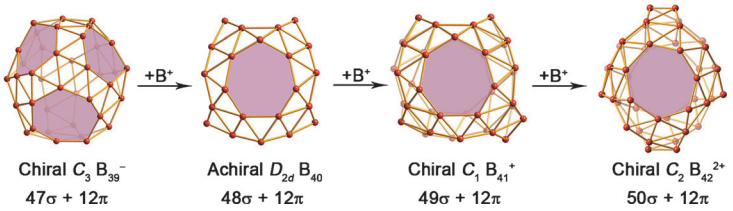

Chiral cations: Following the recently observed C_3/C_2 B_{39}^- and D_{2d} B_{40}, two new chiral members C_1 B_{41}^+ and C_2 B_{42}^{2+} are introduced to the borospherene family. These chiral borospherene cations are composed of twelve interwoven boron double chains with six hexagonal and heptagonal faces and exhibit σ plus π double delocalization, which can be viewed as cuborenes analogous to cubane (C_8H_8).

Lithium–Air Battery

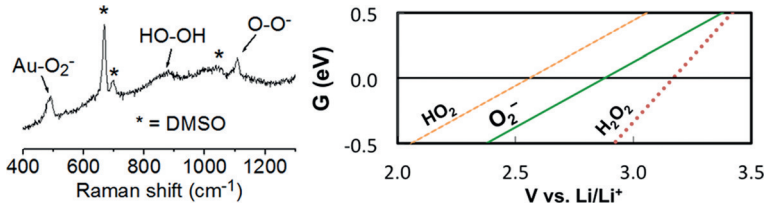

Stable superoxide found in gold ORR: An in situ spectroscopic study of the oxygen reduction reaction (ORR) on gold in a DMSO electrolyte containing phenol as a proton source shows that the ORR can begin with $1e^-$ transfer to O_2. Thus O_2^-, not HO_2, is the first stable intermediate during the ORR to hydrogen peroxide. The unusual stability of O_2^- is explained using DFT calculations.

Conformational Analysis

Fatal attraction: The noncovalent interaction of a hydroxy group with pyrazines and quinoxalines involves a lone pair (lp)–heteroarene attraction which is stronger and solvent independent when measured relative to the π-facial hydrogen bond to a benzene ring. Organic fluorides also prefer the heteroarene ring over benzene. The attraction between a quinoxaline and a terminal alkyne is stronger than an OH–arene interaction.

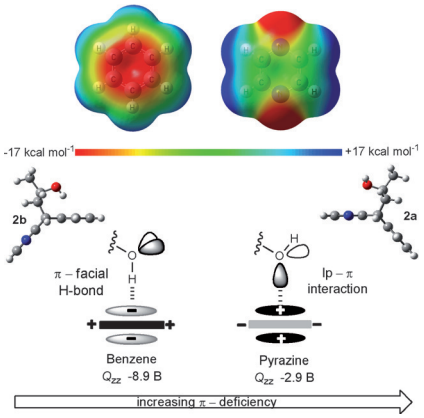

Polycycles

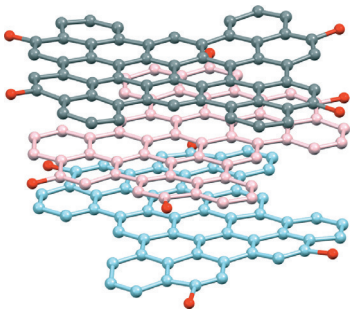

Triple the fun: Synthesis of an all-carbon conjugated tetrabenzoperipentacene was achieved. The single-crystal X-ray structure revealed that the molecules form a triple-layered cluster-like β-graphite. The remarkably rigid carbon framework results in a small Stokes shift and fully reversible five-electron oxidation potentials.

Nanocomposite electrocatalyst: A high-performance electrocatalyst for the oxygen reduction reaction (ORR) is based on Fe_3C nanoparticles encapsulated in mesoporous Fe-N-doped carbon nanofibers. It can be synthesized from low-cost and abundant precursors and exhibits excellent electrocatalytic performance for the ORR in both alkaline and acidic media.

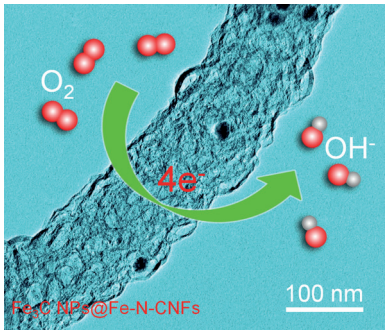

Electrocatalysis

Chemical gardens: Self-assembling membranes in iron sulfide and iron hydroxide reaction systems were studied. The electrical potential and current generated by precipitation of the inorganic membranes were measured. The battery-like properties of the chemical gardens were demonstrated by linking multiple experiments in series, which produced sufficient electrical power to light an external light-emitting diode.

Inorganic Membranes

Hydrogen generation on self-supported three-dimensional nickel phosphide nanosheet array cathodes is reported. The nanosheets have been fabricated by direct phosphorization of commercial nickel foams using phosphorus vapor and show superior electrocatalytic activity and stability in acidic medium toward H_2 generation.

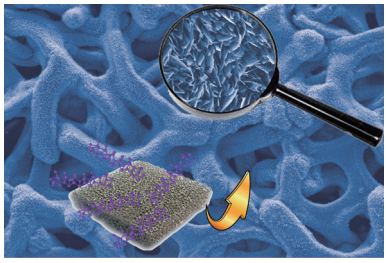

Electrocatalysis

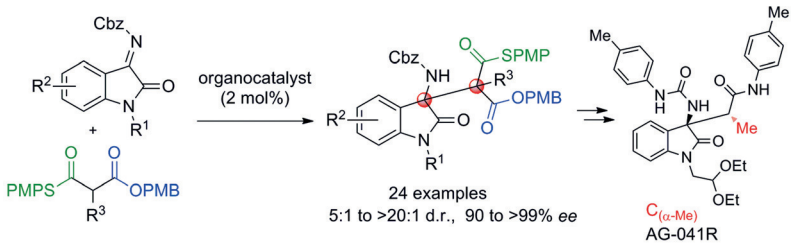

Asymmetric Synthesis

Crowd around: Oxindoles with adjacent fully substituted stereogenic centers were formed by mild organocatalytic addition reactions with high diastereo- and enantioselectivities. The synthetic versatility of the products with orthogonally addressable functional moieties was showcased in the synthesis of derivatives of the bioactive oxindole AG-041R.

Asymmetric Synthesis

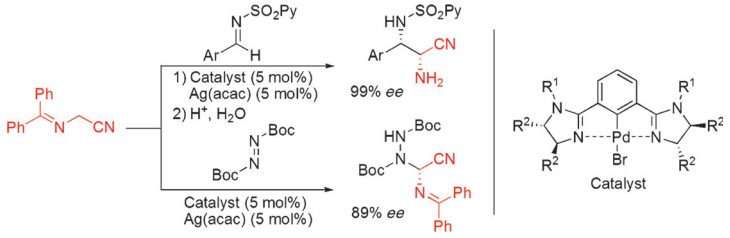

Good yields and diastereo- and enantioselectivities were observed for the title reaction with various imines using chiral bis(imidazoline)/Pd catalysts. The reaction of α-aminonitriles with di-*tert*-butyl azodicarboxylate afforded chiral α,α-diaminonitrile in high yield with high enantioselectivity. acac = acetylacetonate, Boc = *tert*-butoxycarbonyl.

Asymmetric Synthesis

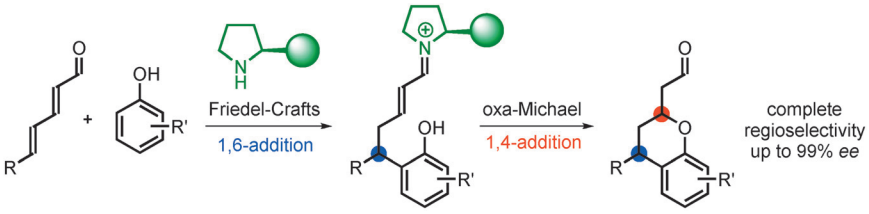

One six one four: Based on a 1,6-Friedel–Crafts/1,4-oxa-Michael sequence, an organocatalyst directs the reaction of hydroxyarenes with a vinylogous iminium-ion intermediate to give only one out of four possible regioisomers. The reaction provides optically active chromans in high yields with up to 99% *ee*.

Perovskites

The influence of light and oxygen on the stability of $CH_3NH_3PbI_3$ perovskite-based photoactive layers is investigated. Upon exposure to both light and dry air, the mesoporous (mp) $Al_2O_3/CH_3NH_3PbI_3$ layers decompose to methylamine, PbI_2, and I_2. This degradation is initiated by the reaction of superoxide (O_2^-) with the methylammonium moiety of the perovskite absorber. MA = methyl ammonium, CB = conduction band, VB = valence band.

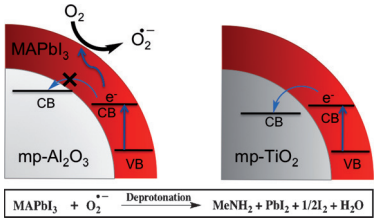

Porphyrinoids

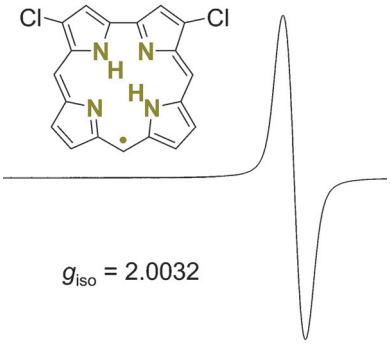

Surprisingly radical was the outcome of an attempt to prepare sterically protected tungsten corroles. Instead of a heavy-metal chelate, a chlorinated corrole radical (see picture) was formed as an air-stable and easy-to-handle open-shell 17π (4*n*+1) porphyrinoid. The loss of one inner H atom results in a planar molecular structure with the ability to bind divalent metal ions, such as zinc(II).

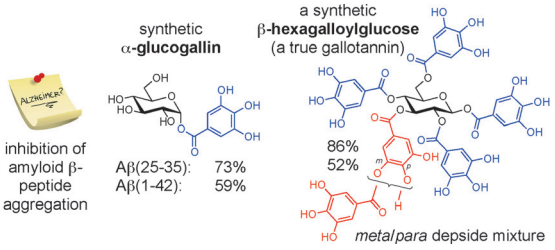

Hexa- and decagalloylglucoses, which belong to the gallotannin plant polyphenols, were chemically synthesized for the first time, and a method for the selective synthesis of the monogalloylglucoses α- and β-glucogallin was developed. An in vitro evaluation showed that the non-natural α-glucogallin and a natural β-hexagalloylglucose are potent inhibitors of amyloid β-peptide aggregation.

Plant Polyphenols

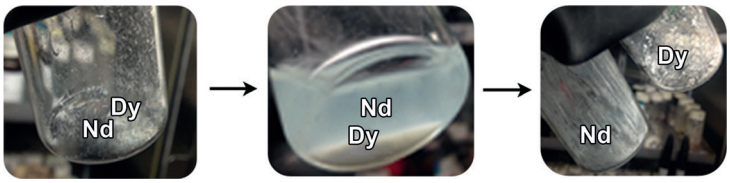

Reuse and recycle: A tripodal nitroxide ligand is used in the separation of Nd and Dy and gives good recoveries from $Nd/Dy(OTf)_3$ mixtures. The separation factor $S_{Nd/Dy} = 359$ achieved is an improvement over conventional separation methods involving liquid–liquid extractions. This method will contribute to incentivizing recycling of Nd/Dy permanent magnetic materials.

Rare-Earth Elements

Take your Pic: Total synthesis of the glycosylated human interleukin-2 (IL-2) has been achieved. The poor solubility of the C-terminal half during purification and ligation was overcome by using the reverse polarity protection of the carboxylic acid by a picolyl (Pic) ester. Together with a new prolyl thioester synthesis for the (28–65) segment, the desired IL-2, having full biological activity, was successfully prepared.

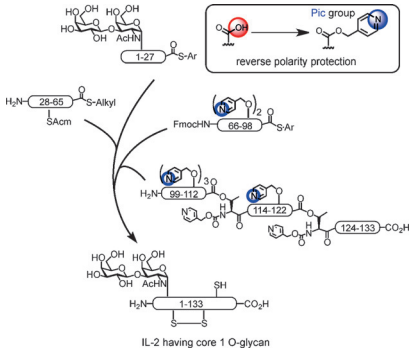

Glycoproteins

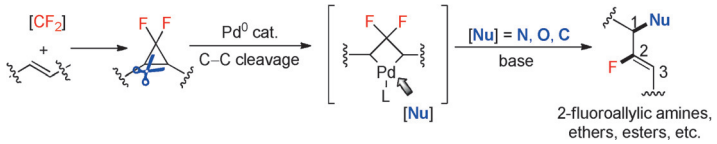

C–C bond cleavage under Pd catalysis induces a regioselective activation of *gem*-difluorinated cyclopropanes. The reaction provides access to a variety of 2-fluoroallylic scaffolds with high *Z*-selectivity and represents the first general application of *gem*-difluorinated cyclopropanes as reaction partners in transition-metal-catalyzed cross-coupling reactions.

Synthetic Methods

Cross-Coupling

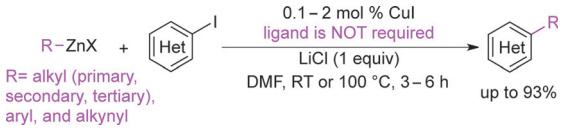

Simply copper: Primary, secondary, and tertiary alkylzinc reagents couple with heteroaryl iodides in the presence of ligand-free CuI without complications arising from β-hydride elimination and rearrangement. The reactions can also be extended to the coupling of aryl- and alkynylzinc reagents. DMF = *N*,*N*-dimethylformamide.

Asymmetric Catalysis

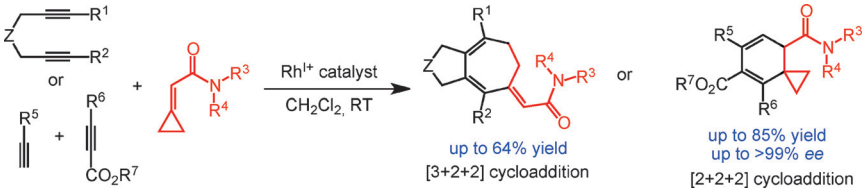

'Cat nap': The cationic Rh^{I}/H_8-binap complex catalyzes the [3+2+2] cycloaddition of 1,6-diynes with cyclopropylideneacetamides to produce cycloheptadienes. In contrast, the cationic Rh^{I}/(*S*)-binap complex catalyzes the enantioselective [2+2+2] cycloaddition of terminal alkynes, acetylenedicarboxylates, and cyclopropylideneacetamides to produce spiro-cyclohexadienes.

Heterocycles

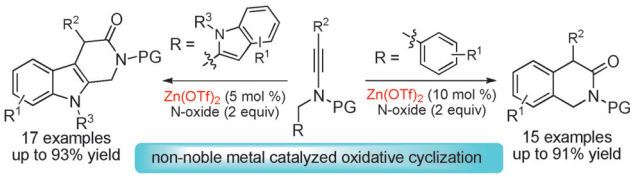

Swap gold for zinc: The title reaction was achieved by a zinc(II)-catalyzed alkyne oxidation/C–H functionalization sequence. In contrast to the well-established gold-catalyzed intermolecular alkyne oxidation, the over-oxidation can be suppressed in this system and the reaction most likely proceeds by a Friedel–Crafts-type pathway. Tf = trifluoromethanesulfonyl, PG = protecting group.

Synthetic Methods

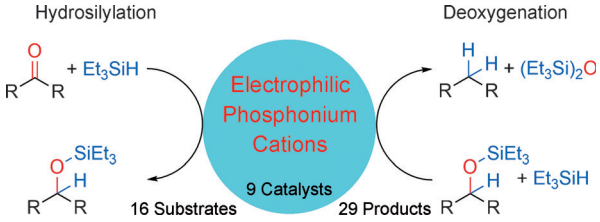

Taking out the O: The salts of the title cations were used in the catalytic stepwise hydrosilylation and deoxygenation of ketones. The dependency of the reaction outcome on Lewis acidity was investigated. In addition, the mechanism of the reduction was probed experimentally as well as with DFT calculations.

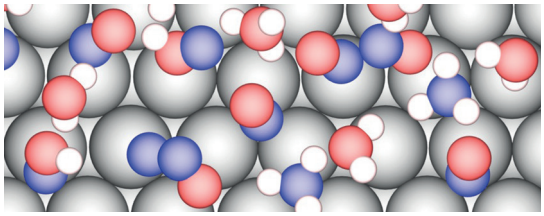

Path finder: The mechanism of nitric oxide electroreduction to ammonia on Pt(111) is investigated using a combination of first principles calculations and electrokinetic rate theories. The results demonstrate that ammonia is produced through a series of water-assisted protonation and bond dissociation steps at modest voltages.

NO Electroreduction

Inside Back Cover

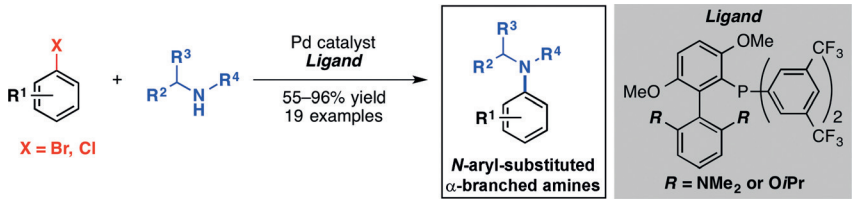

Coupled by design: The arylation of sterically demanding α-branched secondary amines was enabled through the design of new palladium catalyst systems. These catalysts help suppress the undesired β-hydride elimination pathways and are effective for the cross-coupling of a wide array of hindered amine nucleophiles with aryl and heteroaryl electrophiles.

Cross-Coupling

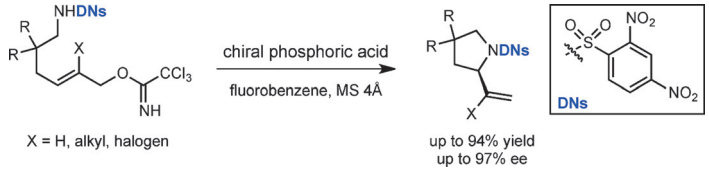

Leaving-group activation: A Brønsted acid catalyzed intramolecular enantioselective S_N2' reaction was developed utilizing trichloroacetimidate as a leaving group. The findings indicated that dual activation of the substrates is operative. This metal-free allylic alkylation allows highly enantioselective access to 2-vinylpyrrolidines bearing various substituents.

Organocatalysis

In a (closed) nut shell: A novel triphenylamine derivative having two phenoxy radicals appended to the amino nitrogen atom has been prepared. This molecule has an unexpected closed-shell electronic state, even at room temperature, in spite of its structural similarity to the galvinoxyl radical. The molecule features two C–N bonds with multiple-bond character and a remarkably low HOMO–LUMO gap.

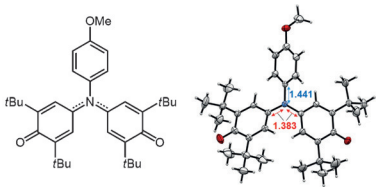

Structure Elucidation

Hydrogenation Reactions

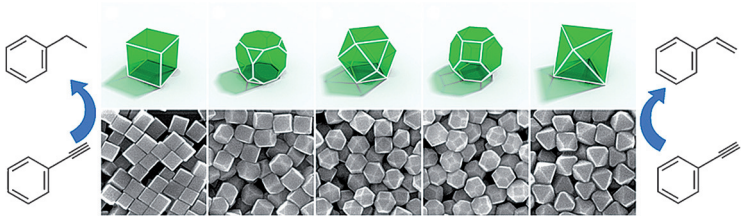

Taking advantage of poisons: The poisoning effect of lead(II) ions can alter the shapes of Pd–Pb alloy nanocrystals. It endows the alloy nanocrystals with superior selectivity for the semihydrogenation of alkynes.

Cesium Fluorides

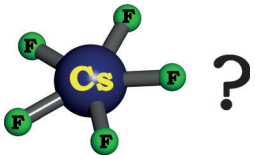

Breaking into cores: Formal core orbitals sometimes may take part in bonding. An instance is provided in theoretical studies of the bonding of CsF_5 (see picture) and CsF_2^+. The results also suggest that these metastable high fluorides of cesium may be experimentally accessible.

Polyfluoride Anions

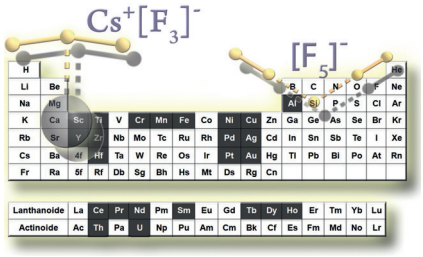

Give me F,F,F,F,F, five: The polyfluoride anions $[F_5]^-$ and $Cs^+[F_3]^-$ have been identified by matrix-isolation spectroscopy and quantum-chemical methods. The V-shaped $[F_5]^-$ ion gives rise to a band found in many IR laser ablation experiments that, up to now, could not be assigned.

Heterocycles

A change of heart: The borazine derivative of hexa-*peri*-hexabenzocoronene was produced in a high-temperature reaction through multiple dehydrogenation of a borazine. The solid-state structure of this BN-doped HBC (BN-HBC) is isotypic with that of the parent HBC. Scanning tunneling microscopy shows that BN-HBC lies flat on Au(111) in a two-dimensional pattern.

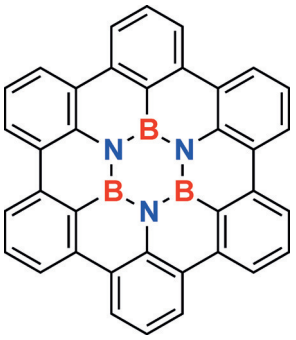

Synthetic Methods

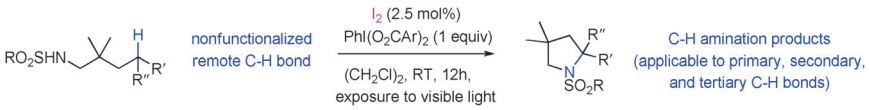

Iodine does it! The first catalytic Hofmann–Löffler reaction proceeds with a combination of catalytic amounts of molecular iodine and a modified hypervalent iodine(III) reagent. The reaction proceeds under mild catalytic conditions and the intramolecular C–H amination addresses primary, secondary, and tertiary C–H groups.

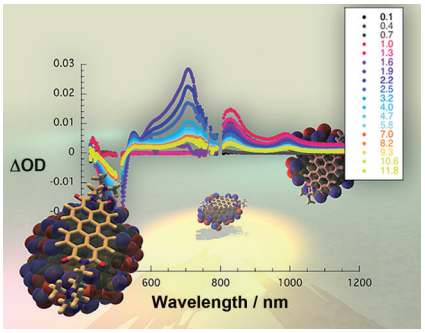

Long-term separation: Charge-transfer complexes formed by electron-donating carbon nanodots and electron-accepting perylenediimides are prepared. In ultrafast pump-probe experiments (see picture) the charge-separated state with a lifetime of 210 ps was found.

Charge Transfer

Supporting information is available on www.angewandte.org (see article for access details).

A video clip is available as Supporting Information on www.angewandte.org (see article for access details).

This article is available online free of charge (Open Access).

This article is accompanied by a cover picture (front or back cover, and inside or outside).

The Very Important Papers, marked VIP, have been rated unanimously as very important by the referees.

The Hot Papers are articles that the Editors have chosen on the basis of the referee reports to be of particular importance for an intensely studied area of research.

Angewandte Corrigendum

The *Journal of the American Chemical Society* article on which this Highlight is based has been retracted (Retraction on "Mechanical Reconfiguration of Stereoisomers" by K. M. Wiggins, T. W. Hudnall, Q. Shen, M. J. Kryger, J. S. Moore, C. W. Bielawski, *J. Am. Chem. Soc.* **2015**, *137*, 3428) based on an investigation conducted by the University of Texas at Austin, which concludes that the data and scientific conclusions of this study are unreliable.
Regardless of the results reported in the retracted publication, the use of force-sensitive functional groups (mechanophores) has become a useful concept of wide applicability. Pulsed sonication is frequently employed to test the mechanochemical response of polymeric materials. In addition, the Highlight provides some valid insights into the mechanisms of sonochemical activation.

Angew. Chem. Int. Ed. **2010**, *49*

DOI: 10.1002/anie.201001360

Angewandte Corrigendum

Figure 1 of this Communication contains a wrong structure for *p*CA. The correct structure is shown below.

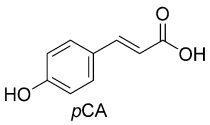

Angew. Chem. Int. Ed. **2015**, *54*

DOI: 10.1002/anie.201500549

Angewandte Corrigendum

Well-Defined Copper(I) Fluoroalkoxide Complexes for Trifluoroethoxylation of Aryl and Heteroaryl Bromides

R. Huang, Y. Huang, X. Lin, M. Rong, Z. Weng* 5736–5739

Angew. Chem. Int. Ed. **2015**, *54*

DOI: 10.1002/anie.201501257

In this Communication, the structure of complex **1a** in Figure 1 contains an error. The correct structure contains two [CF_3CH_2O] moieties, as indicated by a revised X-ray crystal structure. The distinct proton and carbon resonance signals appear in the ^{1}H and ^{13}C NMR spectra of compound, indicative of diamagnetic copper(I) species. Deducing from the charge balance, among two [CF_3CH_2O] groups, one of them is protonated. The cocrystallized CF_3CH_2OH can be removed by washing the complex with diethyl ether and drying under vacuum overnight. The reaction exploiting [Cu(phen)$_2$(CF_3CH_2O)] (with NaO*t*Bu) has shown a similar result to that using [Cu(phen)$_2$(CF_3CH_2O)-(CF_3CH_2OH)] as described in the original paper.

Furthermore, in the Experimental Section, "CF_3CH_2OH (0.60 g, 6.0 mmol)" should be "CF_3CH_2OH (1.20 g, 12.0 mmol)" and "^{1}H NMR (400 MHz, [D_6]DMSO) δ 9.10 (s, 4H), 8.64 (d, J = 7.9 Hz, 4H), 8.12 (s, 4H), 7.89 (s, 4H), 3.86 (s, 2H). ^{19}F NMR (376 MHz, [D_6]DMSO) δ −75.4 (s, 3F)" should be "^{1}H NMR (400 MHz, [D_6]DMSO) δ 11.0 (br, 1H), 9.10 (s, 4H), 8.64 (d, J = 7.9 Hz, 4H), 8.12 (s, 4H), 7.89 (s, 4H), 3.86 (br, 4H). ^{19}F NMR (376 MHz, [D_6]DMSO) δ -75.4 (s, 6F)".

Similarly, **1c** contains about 0.5 molecule of $CF_2HCF_2CH_2OH$ as indicated by the ^{19}F NMR spectrum with *p*-(trifluoromethyl)toluene as an internal standard. For the synthesis of **1c**, "$HCF_2CF_2CH_2OH$ (0.78 g, 6.0 mmol)" should be "$HCF_2CF_2CH_2OH$ (1.56 g, 12.0 mmol)".

In the Supporting Information, on page S4, for the ^{13}C NMR data of **1b**, "155.1 (s), 155.0 (s), 154.9 (s)" should be "155.0 (m)".

The authors would like to acknowledge Dr. Peter Mueller and Dr. Fang Wang at the Massachusetts Institute of Technology for pointing out these errors which do not affect the main conclusions of the work.

